JOURNAL OF MATERIALS SCIENCE **34** (1999) 5983–5987

Preparation and characterization of mesoporous titania gel-monolith

BAODIAN YAO, LIDE ZHANG
Institute of Solid State Physics, Academia Sinica, P.O. Box 1129, Hefei 230031, People's Republic of China
E-mail: nanolab@mail.issp.ac.cn

This paper focused on the preparation and characterization of a pure TiO_2 monolith. The preparation method is based on the sol-gel technique using tetrabutyl titanate as precursors. By controlling the hydrolysis of tetrabutyl titanate and the rate of gel drying, transparent TiO_2 gel-monoliths are obtained at room temperature. The TiO_2 gel-monoliths prepared in this manner have a mean pore diameter about 4.4 nm, specific surface area 332.8 m^2g^{-1} and more than 57.6% porosity, especially, the TiO_2 gel-monoliths are not amorphous but crystalline, anatase phase. It retains a surface area and a porosity of about 90.5 m^2g^{-1} and 45.6%, respectively, after the heat treatment at 500 °C for 2 h. And XRD, TEM and N_2 adsorption isotherm analysis indicate that particle growth is the main influencing factor of the specific surface area and porosity from room temperature to 500 °C, but from the heat treatment temperature higher than 500 °C, the densification assisted by anatase to rutile phase transition become the main role to influence the specific surface area and porosity.

1. Introduction

Nanostructured porous materials not only have been widely used in the field of separation, catalysis, gas sensing and electrolyte [1–4], but also have received considerable attentions as hosts or matrices in the developing field of preparing nanotubes [5], nanorods [6], and composites [7–10]. In almost all of these, the size of the pores, the value of specific surface area (SSA) and porosity are important factors for the performance of above materials. Therefore, it is of fundamental interest to prepare porous monolithic materials with high SSA, porosity, and nanosized pores with a narrow pore size distribution.

A search of the literatures indicates that preparations of TiO_2 powders and films have been widely reported [11–14]. There are also reports about the preparation of monolithic TiO_2 composite systems, such as TiO_2-SiO_2 [15–16] and PbO-TiO_2 [17], while the preparation of a pure TiO_2 monolith has not been well studied.

Because of the advantages of the sol-gel method, it is often employed to prepare gels or glasses. However, when it is employed to prepare pure TiO_2 monoliths, there are two major problems: one is the fast hydrolysis of the titanium precursor; the other is the destabilization of the alcogel [18] in the aging and drying process. Those two problems are not exist in the SiO_2 [19] or ZrO_2 [20] systems. In the only published articles [21–22] reporting the formation of alkoxide-derived (sol-gel) TiO_2 monoliths with amorphous structure at room temperature, special experimental conditions were needed to solve these two problems. In this paper, without using special experimental conditions, just by reducing the hydrolysis rate with ice water and keeping the drying temperature constant at room temperature, we prepared transparent anatase mesoporous TiO_2 monoliths successfully. The purpose of this paper is to add to the body of knowledge which might assist in the preparation of these monolithic materials.

2. Experimental

2.1. Sample preparation

Tetrabutyl titanate is used as the precursor compound for the sol-gel process to obtain TiO_2. To reduce the hydrolysis rate, 20 ml tetrabutyl titanate was first added to a mixture of 10 ml acetic acid and 40 ml butyl alcohol to form solution (a), and then 4.5 ml deionized water in the form of ice was added to solution (a) under furious magnetic stirring with a teflon coated magnetic stirrer for an hour at room temperature, and a clear, amber solution (b) was obtained. Solution (b) was cast in a glass vessel covered with a plastic film having pin holes and formed transparent gel after 12 h at room temperature. During the subsequent aging process, the liquor emerged in the vessel was drawn out with a needle tube. After about 30 days, the gel was further heated at 40 °C for ten days to obtain as prepared gel-monoliths. These gel-monoliths were then fired at various temperatures in air, the heating rate for all samples was 20 °C/h, and all samples were held at the peak firing temperatures for 2 h and then cooled naturally.

2.2. Sample characterization

The differential scanning calorimetry (DSC) analysis of the as prepared TiO_2 gel-monoliths was conducted

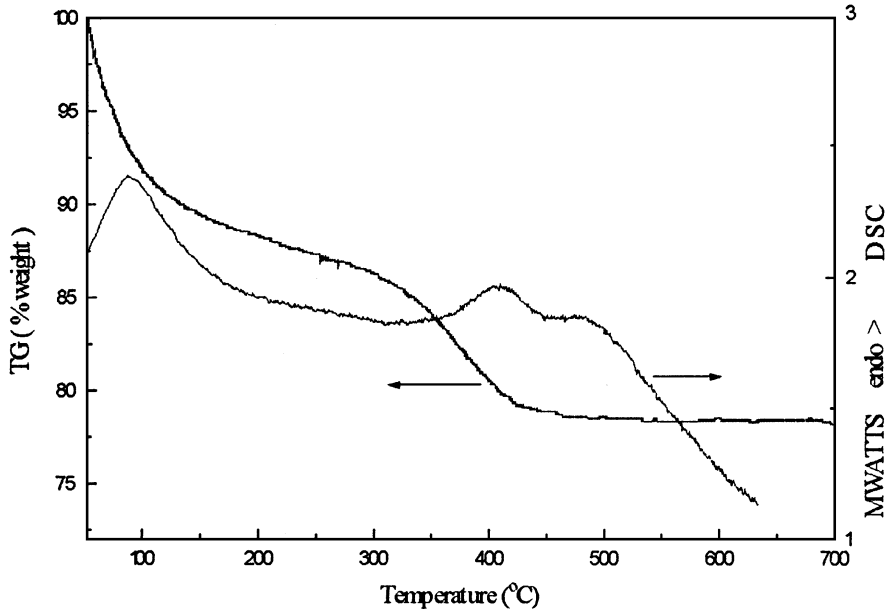

Figure 1 Thermal analysis of TiO_2 sample as prepared.

in high-pure N_2 with a Perkin-Elmer DSC-2 differential scanning calorimeter and thermal gravimetry (TG) was carried out in Perkin-Elmer TGA- 2 thermal gravimeter in air, both measurements were at a heating rate of 10 °C/min. The X-ray diffraction (XRD) powder patterns obtained on a Phillips Pw 1700 X-ray Diffractometer using CuK_α radiation at a scan rate of $0.06^\circ\ 2\theta\ S^{-1}$ were used to determine the identity of any phase present and their crystallite size. The crystallite size was calculated from X-ray line-broading analysis by Scherrer formula. Phase identification and crystallite size measurements were further corroborated by transmission electron microscopy (TEM) using a JEM-200cx apparatus operating at 200 KV.

Nitrogen-gas physisorption measurements of all the samples were conducted at liquid-nitrogen temperature using Micromeritics ASAP 2000 apparatus. All the samples measured were degassed at 110 °C before the actual measurements. The specific surface area and pore size distribution were directly given by the computer annexed to the apparatus. The porosity, from the saturation adsorption volume of nitrogen-gas (standard temperature and pressure or STP) obtained from the adsorption branch of the isotherm, was calculated by the relation (the skeleton specific volume of anatase TiO_2 is taken as 0.27 cm^3g^{-1}),

$$P = \frac{V_p}{V_p + 0.27} \tag{1}$$

$$V_p = 1.547 \times 10^{-3} V_d \tag{2}$$

where V_p is the volume of the liquidated nitrogen corresponding to the total pore volume, which was calculated from the saturation adsorption volume in STP, Vd. The particle size D_{SSA} was calculated by the expression,

$$D_{SSA} = \frac{6}{\rho \times SSA} \tag{3}$$

according to the equivalent spherical model, where ρ is the skeleton density of anatase TiO_2 taken as 3.75 gcm^{-3}, and SSA is the specific surface area.

3. Result and discussion

3.1. Thermal analysis

TG-DSC results of the TiO_2 samples as prepared are illustrated in Fig. 1. As can be seen from the TG curve, there are two regions of mass loss (21.56% in total), associated with two endothermic DSC peaks at 85 and 408 °C. The mass loss up to 270 °C corresponds to the desorption of absorbed water and residual butyl alcohol embedded in the pores (13.28%), between 270 and 470 °C, the mass loss corresponds to the removal of the residual unhydrolysed organic (8.28%), there are no exothermic peaks on DSC curve in the temperature range from 50 to 640 °C that we measured, which indicates no crystallization or phase transition occurred in this temperature range.

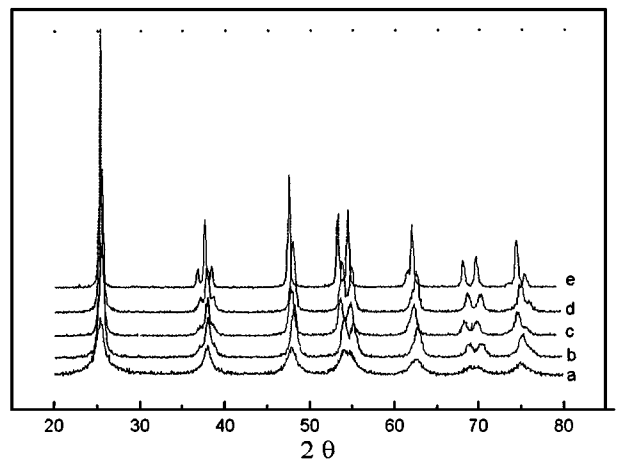

Figure 2 X-ray diffraction patterns of TiO_2 samples. (a) as prepared, (b) 300 °C, (c) 400 °C, (d) 500 °C, (e) 600 °C.

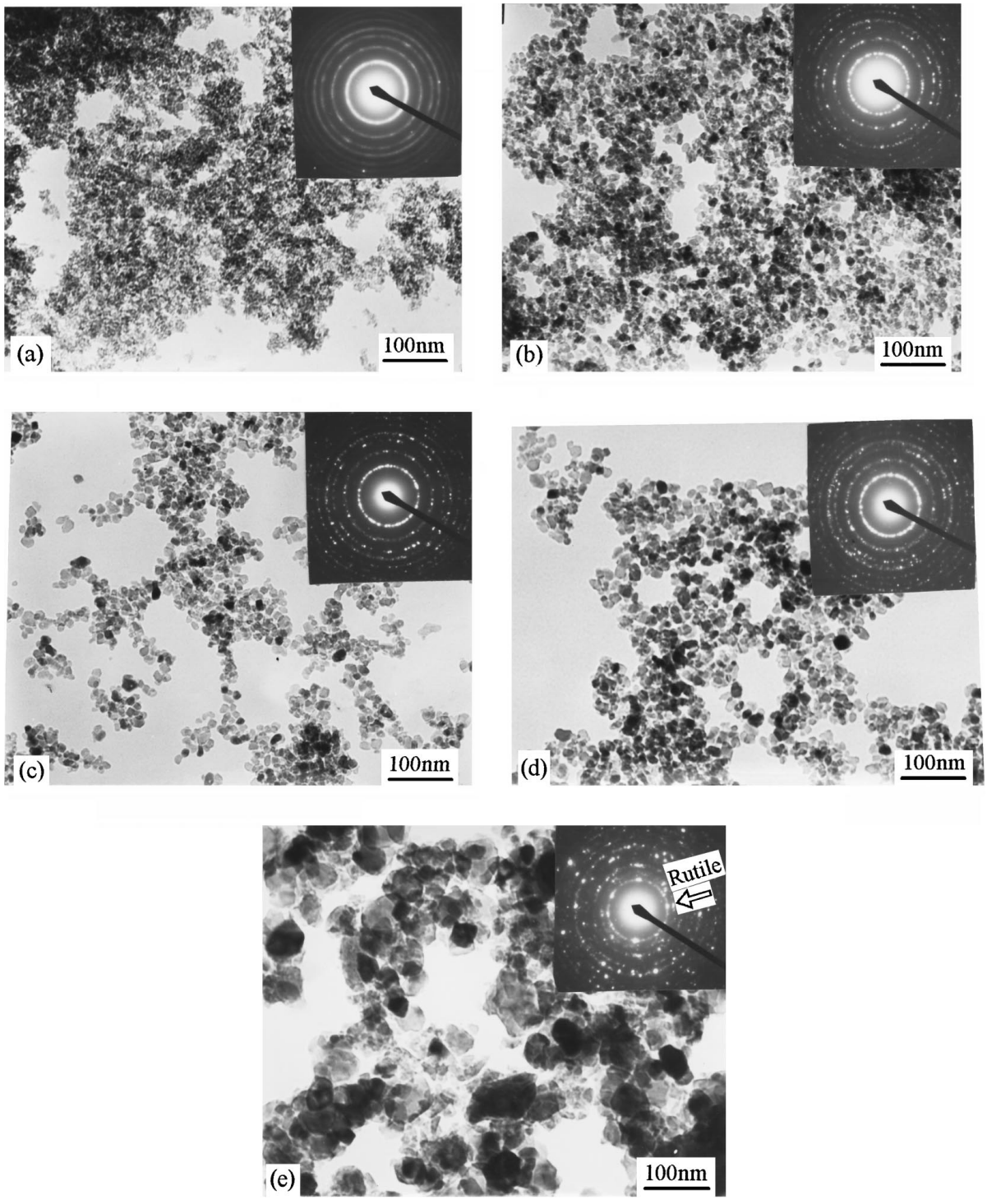

Figure 3 TEM graphs and SAED patterns. All the diffraction rings correspond to the anatase phase unless the marked one (rutile). (a) as prepared, (b) 300 °C, (c) 400 °C, (d) 500 °C, (e) 600 °C.

3.2. Crystal structure

The results of XRD and TEM both prove the TiO_2 samples as prepared are crystalline, anatase phase, as indicated by the presence of crystalline peaks in Fig. 2a and the presence of anatase diffraction ring in Fig. 3a, respectively. All the peaks in Fig. 2 correspond to the anatase phase of titania, no rutile phase appeared even for the sample calcined at 600 °C, however, rutile phase can be seen in Fig. 3e, as indicated by the presence of rutile diffraction ring appeared in Fig. 3e, and this result shows that phase transition of anatase to rutile occurs for the sample calcined at 600 °C. But the fact that the result of TEM in disagreement with that of XRD shows that either the crystal size or the amount of the rutile phase is small. Upon heating, as can be seen from Fig. 3a to Fig. 3e, the particles grow slowly and homogeneously, but serious and inhomogeneous growth occurred for the samples calcined at 600 °C. Furthermore, the fact that phase transition of anatase to rutile occurred over this temperature range maybe contribute to the inhomogeneous particle growth by providing the heat of transformation. The good agreement between D_{XRD} and D_{TEM} (see Table I), which is determined by counting the number of particles having a given size in

TABLE I Particle size from different measurements: XRD, TEM, SSA

Temperature (°C)	D_{XRD} (nm)	D_{TEM} (nm)	D_{SSA} (nm)
as prepared	6	6.5	4.8
300	10.3	10.7	13.1
400	10.3	11.5	13.7
500	14.9	15.6	17.9
600	29.8	31.4.	64.9

TABLE II SSA, porosity and mean pore diameter of titania samples

Temperature (°C)	SSA (m^2g^{-1})	Porosity (%)	Mean pore diameter (nm)
as prepared	332.8	57.6	4.4
300	123.7	54.4	10.4
400	118.4	53.6	10.5
500	90.5	45.6	10
600	25	18.6	9.8

a given area, indicates that the particles of TiO_2 monoliths are just packed together with soft aggregation.

3.3. Pore structure

Fig. 4 shows the full sorption isotherm and pore size distribution diagrams of TiO_2 as prepared. This is a typical IV isotherm, indicating that the pores of sample are mesopores. On the basis of Zsigmondy model [23], the isotherm can be explained as follows. Along the initial part of the adsorption isotherm, adsorption is restricted to a thin layer on the wall of pores until the relative pressure increased to 0.42 (the inception of the hysteresis loop) and the condensation of nitrogen begins in the finest pores and almost all pores are full of liquidated nitrogen when the relative pressure increased to 0.85 (the end of the hysteresis loop). During the desorption process, fast desorption occurs when the relative pressure is reduced to 0.6. This adsorption-desorption measurement shows that the pores of the sample are interconnected. According to the Wheeler equation [24], the pore diameters corresponding to the relative pressure 0.42, 0.6 and 0.85 are 3.7, 5.6 and 14.4 nm, respectively. From the pore size distribution curve of Fig. 4, we can see that the pore size distribution is narrow and most pores fall into the range of 3.5–7 nm in diameter. Considering the above analysis, we can conclude that the pores are mesoporous and interconnected, and the whole pore volume is mainly ascribed to those pores whose diameters are between 3.5 and 7 nm, with mean pore diameter 4.4 nm.

3.4. Effect of heat treatment on SSA and porosity

As we know, porosity (%) is directly associated with particle packing density, while the specific surface area is a function of the particle size and packing density; and particle packing density, in turn, associated with densification. In the temperature range from room temperature to 500 °C, the fact that the porosity (see Table II) changes a little means the particle packing density (or densification) changes a little, and thus the change of SSA is mainly influenced by the growth of particles (see Table I). When the heat treatment temperature is higher than 500 °C, the fact that the dramatic decline in porosity and SSA shows that sintering in some extent occurred and densification becomes the main influencing factor of SSA and porosity. The disagreement of the D_{SSA} with the D_{XRD} data in such a degree for the sample calcined at 600 °C means some closed pores begin to form as a result of densification. The rutile phase appear at 600 °C as indicated by SAED result (Fig. 3e) can be used, according to Kumar *et al* [25], to express the anomaly of particle growth, of the decline of porosity and SSA because of the phase transformation of anatase to rutile which assists in the densification process.

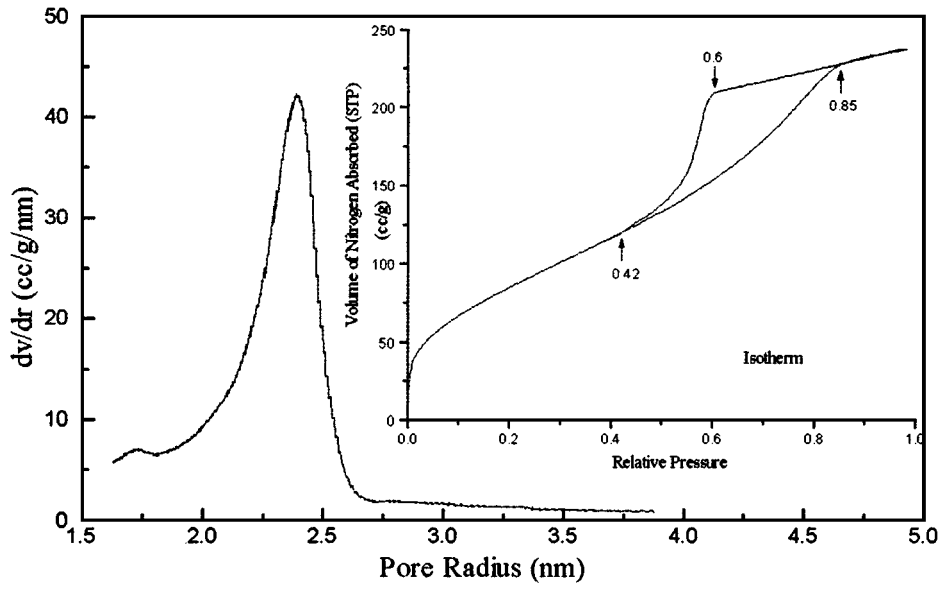

Figure 4 Full sorption isotherm and pore size distribution diagram of TiO_2 sample as prepared.

4. Summary

Transparent, mesoporous anatase TiO_2 monoliths are synthesized by sol-gel method using tetrabutyl titanate as precursor. The preparative procedure includes producing a clear sol which can be stable for several hours. These sols are kept in a vessel covered with a plastic film having pin holes for aging at room temperature. Through gelation and slowly gel drying, TiO_2 gel-monoliths are obtained in this manner. N_2 adsorption isotherm studies indicates that the pores of TiO_2 gel-monoliths as prepared display mesoporous features with large porosity. The mean pore diameter of TiO_2 falls into mesoporous region.

Upon heating, XRD, TEM and N_2 adsorption isotherm analysis indicate that, from room temperature to 500 °C, the SSA and porosity are mainly influenced by particle growth, the contribution of densification of the SSA and porosity is negligible. When the heat treatment temperature rises to 600 °C, densification assisted by anatase to rutile phase transition becomes the main role influencing the SSA and porosity changes.

References

1. M. A. ANDERSON, M. J. GIESELMANN and Q. XU, *J. Membrane. Sci*. **39** (1988) 243.
2. G. M. PANJONK, *Appl. Catal*. **72** (1991) 217.
3. YUAN-CHANG YEH, TSEUNG-YUEN TSENG and DEH-AU CHANG, *J. Amer. Ceram. Soc*. **72** (1989) 1472.
4. YAO-CHUN SHEN, LIN WANG, ZUHONG LU, YU WEI, QINGFU ZHOU, HAIFANG MAO and HUIJUN XU, *Thin Solid Films* **257** (1995) 144.
5. W. Z. LI, S. S. XIE, L. X. QIAN, B. H. CHANG, B. S. ZOU, W. Y. ZHOU, R. A. ZHAO and G. WANG, *Science* **274** (1996) 1701.
6. G. W. MENG, L. D. ZHANG, C. M. MO, S. Y. ZHANG, Y. QIN, S. P. FEN and H. J. LI, *Solid State Communications* **106** (1998) 215.
7. WEIPING CAI, MING TAN, GUOZHONG WANG and LIDE ZHANG, *Appl. Phys. Lett.* **69** (1996) 2980.
8. WEIPING CAI, HUICAI ZHONG and LIDE ZHANG, *J. Appl. Phys*. **83** (1998) 1705.
9. T. J. GOODWIN, V. J. LEPPERT, C. A. SMITH, S. H. RISBUD, M. NIEMEYER, P. P. POWER, H. W. H. LEE and L. W. HRUBESH, *Appl. Phys. Lett*. **69** (1996) 3230.
10. T. K. KUNDO, M. MUKHERJEE, D. CHAKRAVORTY and T. P. SINHA, *J. Mater. Sci*. **33** (1998) 1759.
11. M. GOPAI, W. J. MOBERIY CHAN and L. C. DE JONGHE, *ibid*. **32** (1997) 6001.
12. JAROSLAV SLUNEČKO, MARIJA KOSEC, JANEZ HOLC and GORAN DRAŽIČ, *J. Amer. Ceram. Soc*. **81** (1998) 1121.
13. Y. PAZ, Z. LUO, L. RABENBERG and A. HELLER, *J. Mater. Res*. **10** (1995) 2842.
14. V. J. NAGPAL, R. M. DAVIS and S. B. DESV, *ibid*. **10** (1995) 3068.
15. J. H. LEE, S. Y. CHOI, C. E. KIM and G. D. KIM, *J. Mater. Sci*. **32** (1997) 3557.
16. B. E. YOLDAS, *J. Non-cryst. Solids*. **38** (1980) 81.
17. YUJI KATAGIRI, HIROYUKI NASU, JUN MATSUOKA and KANICHI KAMIJA, *J. Amer. Ceram. Soc*. **77** (1994) 673.
18. DONG JIN SUH and TAE-JIN PARK, *J. Mater. Sci. Lett*. **16** (1997) 490.
19. S. SAKKA and K. KAMIYA, *J. Non-cryst. Solids* **42** (1980) 403.
20. J. C. DEBSIKDAR, *ibid*. **86** (1986) 231.
21. YOSHIMI TANAKA, HIROYUKI HIRAKAWA and MASAYUKI NOGAMI, *J. Ceram. Soc. Japan*. **102** (1994) 578.
22. QUNYIN XU and MARC A. ANDERSON, *J. Amer. Ceram. Soc*. **77** (1994) 1939.
23. S. J. GREGG and K. S. W. SING, "Adsorption, Surface Area and Porosity" (Academic, London,1982) chap. 3.
24. A. WHEELER, *Catalysis* **2** (1955) 116.
25. K-N. P. KUMAR, K. KEIZER, A. J. BURGGRAAF, T. OKUBO, H. NAGAMOTO and S. MOROOKA, *Nature* **358** (1992) 48.

Received 26 January
and accepted 23 June 1999